Additive noise effects in active nonlinear spatially extended systems

M. PRADAS [1], G.A. PAVLIOTIS [2] S. KALLIADASIS [1],

D.T. PAPAGEORGIOU [2], and D. TSELUIKO [3],

[1] *Department of Chemical Engineering, Imperial College London, London, SW7 2AZ, UK*

[2] *Department of Mathematics, Imperial College London, London, SW7 2AZ, UK*

[3] *School of Mathematics, Loughborough University, Leicestershire, LE11 3TU, UK*

(*Received 5 April 2012*)

We examine the effects of pure additive noise on spatially extended systems with quadratic nonlinearities. We develop a general multiscale theory for such systems and apply it to the Kuramoto-Sivashinsky equation as a case study. We first focus on a regime close to the instability onset (primary bifurcation), where the system can be described by a single dominant mode. We show analytically that the resulting noise in the equation describing the amplitude of the dominant mode largely depends on the nature of the stochastic forcing. For a highly degenerate noise, in the sense that it is acting on the first stable mode only, the amplitude equation is dominated by a pure multiplicative noise, which in turn induces the dominant mode to undergo several critical state transitions and complex phenomena, including intermittency and stabilisation, as the noise strength is increased. The intermittent behaviour is characterised by a power-law probability density and the corresponding critical exponent is calculated rigorously by making use of the first-passage

properties of the amplitude equation. On the other hand, when the noise is acting on the whole subspace of stable modes, the multiplicative noise is corrected by an additive-like term, with the eventual loss of any stabilised state. We also show that the stochastic forcing has no effect on the dominant mode dynamics when it is acting on the second stable mode. Finally, in a regime which is relatively far from the instability onset, so that there are two unstable modes, we observe numerically that when the noise is acting on the first stable mode, both dominant modes show noise-induced complex phenomena similar to the single-mode case.

Key Words: Stochastic partial differential equations, critical phenomena, multiple scale methods, singular perturbations.

---

1 Introduction

External or internal random fluctuations are ubiquitous in many physical systems and can play a key role in their dynamics often inducing a wide variety of complex spatio-temporal phenomena. Examples can be found in several fields: From biology (such as stochastic resonance accounting for the sensitivity that certain species have, to weak but coherent signals in noisy environments) and technological applications (e.g. high-temperature superconductivity [2, 52]), to fluid dynamics (e.g. Rayleigh-Bénard convection commonly used as a prototype to study instabilities in systems out of equilibrium [7], contact line dynamics [55] and waves in free-surface thin film flows [23, 42]). Many of these natural phenomena and technological applications can be described by model noisy spatially extended systems (SES), i.e. infinite-dimensional dynamical systems described through

stochastic partial differential equations (SPDEs) with space-time dependence [45], such as the noisy Swift-Hohenberg equation, or the noisy Kuramoto-Sivashinsky (KS) equation. The spatio-temporal dynamics of noisy SES can be dominated by many curious phenomena, such as noise-induced spatial patterns [13] and noise-induced phase transitions [16]. Clearly, characterising the influence of noise in SES is crucial for the understanding of the inception and long-time complex spatio-temporal dynamics of physical systems, as well as for the control and optimisation of technological processes. The identification and understanding of different regimes in parameter space, including the emergence of underlying scaling laws is of particular interest in analytical and computational studies of such systems.

One of the most widely studied complex phenomena induced by noise effects is the transition between different observed system states as the noise strength is continuously increased beyond a critical value. A related question concerns the mechanisms by which fluctuations in the system interact with nonlinearities to induce ordered or regularised states (see [14, 45]). It is now generally accepted that one of the main mechanisms required to induce phase transitions (e.g. between ordered-disordered phases), is the presence of pure multiplicative noise[1], even though the presence of combined multiplicative and additive noise has also been shown to induce phase transitions [26, 56]. On the other

[1] Multiplicative noise enters the system through external effects, i.e. via the presence of noise on a controlling parameter or through noisy fluctuations in the boundary conditions; on the other hand, additive noise arises from fluctuations of an internal origin such as thermal fluctuations, which although they are present at the nanoscale, they can often have macroscopic effects (e.g. [33]).

hand, complex phenomena such as stabilisation effects (but not phase changes) can be induced by pure additive noise as reported in recent numerical investigations [17, 18, 34].

In this study, we investigate the effects of pure additive noise on unstable SES that are close to the primary bifurcation ("instability onset"). A first stab at this problem was our recent study in [41] which focused on the influence of highly degenerate noise, a particular type of additive noise, on the KS equation – the noisy KS equation is a paradigmatic model for a wide spectrum of physical settings. In [41] it was shown that being close to the instability onset allows for a global description of the KS equation in terms of a single dominant mode. In the present work, by means of a multiple scale analysis for general SES with quadratic nonlinearities and by appropriately extending the singular perturbation methodology in [38] for such SES, we obtain an amplitude equation for the dominant mode which then enables us to describe analytically the behaviour of this mode and explore systematically the effects of noise. As an application of the general methodology we examine the noisy KS equation. We offer a derivation of this equation for a hydrodynamic system, that of a thin-liquid film flowing over a topographical substrate obtained asymptotically from governing equations (Navier-Stokes) and wall and free-surface boundary conditions. In other contexts, the noisy KS equation has been adopted, for instance, as a model for sputtering processes used to produce thin films in materials applications including nanostructuring solid surfaces using ion beam erosion – in addition, a possible use of noise as a control tool is also suggested and explored computationally, see [8, 12, 27, 29, 30].

We observe that the dynamics, and in particular the statistical properties of the fluctuating dominant mode, are largely dependent on the nature of the applied noise and

its strength. More precisely, we consider a degenerate noise, in the sense that it is acting on the subspace of stable modes alone, and scrutinise its effects on the dynamics of the unstable mode. Several situations arise depending on what stable mode (or modes) the noise is acting on. For example, when the noise is acting on the first stable mode only, the governing equation for the amplitude of the dominant (unstable) mode is reduced to a purely temporal Stuart-Landau (SL) model with pure multiplicative noise. The numerical simulations presented in our previous study [41] suggested that this type of noise is in turn responsible for the different critical transitions that the dominant mode undergoes as the noise strength is increased, including an initial state of finite fluctuations, an intermittent on-off state characterised by a burst-like dynamics, and a completely stabilised state. It is noteworthy that such critical transitions exhibit universal underlying scaling laws, in the sense that the observed critical exponents are also ubiquitously found in many different physical systems. It is also noteworthy that such observed on-off intermittency is actually a crucial feature of many nonlinear systems close to criticality, and reflects a transition from order/coherence to a disordered state.

Here, we rigorously derive the statistical properties of such intermittency in terms of a universal law that does not depend on the particular model under consideration. We further offer new results and insights on the influence of noise on SES compared to our previous study in [41]. More specifically, when the noise acts on the whole set of stable modes, we show that the multiplicative term in the SL equation is corrected by an additive-like term, and any stabilisation effect is eventually lost. Additionally, we find that the noise can be filtered out by the nonlinearities when it is acting on the second stable mode alone. In this case, the dynamics of the dominant mode is not affected by

the stochastic forcing applied to the system. Our analytical findings are in full agreement with numerical experiments of the KS equation, thus providing a complete picture of the relevant effects of additive noise on SES with quadratic nonlinearities close to the instability onset.

Following the development of analytical and computational descriptions of the phenomena near the primary bifurcation point, it is important to consider the dynamics beyond criticality where the multiscale analysis is no longer valid. To achieve this we revert to numerical experiments and compute the resulting spatio-temporal dynamics when two linearly unstable modes are active. Surprisingly, when we consider a highly degenerate noise acting on the first stable mode alone, the dynamics of the two dominant modes are found to follow the same critical transitions as with the case close to the primary bifurcation where only one unstable mode is present.

In §2 we present the theoretical framework for noisy SES close to the primary bifurcation. In §2.1 we derive the generic amplitude equations for the unstable mode components using multiscale techniques. Our theory is then applied to the noisy KS equation in §3, and both analytical and numerical results for the different cases of noise considered are presented in §3.1, where we take the noise acting on the first stable mode only, in §3.2, where the noise acts on the first and second stable modes, and in §3.3, where the noise acts on the second stable mode only. A numerical study in a regime relatively far from the instability onset is presented in §4. Finally, our results are summarised in §5.

2 Theoretical framework: Noisy SES close to the primary bifurcation

Typically, noisy SES can be described through SPDEs of the following generic form:

$$\partial_t u = \mathcal{L}u + \mathcal{F}(u, \nabla u, \nabla^2 u, \ldots) + \tilde{\sigma}\xi(\boldsymbol{r}, t), \tag{2.1}$$

where $\mathcal{L}$ is usually a linear differential operator with constant coefficients, and $\mathcal{F}$ is a nonlinear function of its arguments. The field $u(\boldsymbol{r}, t)$ describes the magnitude of a quantity of interest in the system, and we also include the presence of a stochastic additive forcing, given by the random variable $\xi(\boldsymbol{r}, t)$, with $\tilde{\sigma}$ its strength. The complexity of SES of the form (2.1) and their dynamics[2] is such that it is often quite difficult, if not impossible, to analyse them directly either analytically or even numerically. It is therefore desirable to obtain an appropriate low-dimensional description representing the dynamics at a coarse-level and which can capture most, if not all of the essential dynamic features of the original high-dimensional model describing the actual problem.

Quite often in physical systems, the dominant nonlinearity is a quadratic one whose functional form is dictated by simple symmetry considerations. For example, in the context of free-surface thin-film flows, the dominant nonlinearity is $u\partial_x u$, associated with the interfacial kinematics due to mean flow [46] (the only other dominant nonlinearity, u^2, is easily ruled out for systems whose spatial average is conserved, i.e. $\partial_t \langle u \rangle_x = 0$). We then consider SES with a quadratic nonlinearity, random forcing and a spatially uniform

[2] It should be emphasised, that already in the absence of noise ($\tilde{\sigma} = 0$), the presence of a wide range of spatial and temporal scales coupled with each other through nonlinearities may give rise to a complex dynamics such as transitions between different patterns and spatio-temporal chaos [7].

rest state. The spatial domain is taken to be $[-L, L]^d$ where $d+1$ is the number of space and time dimensions. We note that even though the multiscale techniques we shall be developing in this study could, in principle be extended to multidimensional systems, this extension is non-trivial and beyond the scope of the present study (in fact, the theory of SPDEs in dimensions higher than one is currently not well developed, at least for space-time white noise). For this reason, we will consider Eq. (2.1) in one spatial dimension ($d = 1$). We also assume that zero is an eigenvalue of the linear operator $\mathcal{L}$ with the corresponding eigenspace being finite dimensional, and the remaining eigenvalues being in the left complex half-plane.

Let us introduce a bifurcation parameter ϵ, such that for $\epsilon = 0$ the system approaches its rest state as $t \to \infty$. For $\epsilon > 0$, a bifurcation occurs leading to a finite number of modes that are linearly unstable. Therefore, we assume that $\mathcal{F}(u, \nabla u, \nabla^2 u, \ldots) = \epsilon^2 \mathcal{J} u + \mathcal{B}(u, u)$, where $\mathcal{J}$ and $\mathcal{B}(u, u)$ are a linear differential operator with constant coefficients and a quadratic nonlinearity (a symmetric bilinear map), respectively, so that for $\epsilon \ll 1$, there appears at least one eigenvalue of the perturbed operator $\mathcal{L} + \epsilon^2 \mathcal{J}$ in the right half-plane. Equation (2.1) is then written in the form:

$$\partial_t u = \mathcal{L} u + \epsilon^2 \mathcal{J} u + \mathcal{B}(u, u) + \epsilon \sigma \xi(x, t). \tag{2.2}$$

For the particular distinguished limit that we will consider in this paper, and which leads to the most interesting coarse-grained dynamics, we have rescaled the noise term in Eq. (2.1) with $\tilde{\sigma} = \epsilon \sigma$ so that its strength is of $O(\epsilon)$, in comparison to the $O(\epsilon^2)$ distance from criticality. Different distinguished limits, relevant when different assumptions on the nonlinearity and the structure of the noise are made, can also be considered, e.g. [3, 6].

The field u can then be projected onto the set of eigenfunctions $\{\mathrm{e}_k(x)\}$ for $k = 1, \ldots, \infty$ of the linear operator $\mathcal{L}$, i.e. $u(x,t) = \sum_k \hat{u}_k(t)\mathrm{e}_k(x)$. For $0 < \epsilon \ll 1$, the system is close to the bifurcation point and is described by the presence of a finite number of unstable modes, the "dominant modes". In this regime, Eq. (2.2) has two widely separated time scales, corresponding to the (stable) fast and (unstable) slow modes, allowing us to derive an amplitude equation for the slow-dynamics of the dominant modes only, which belong to the null space $\mathcal{N}$ of the linear operator $\mathcal{L}$.

2.1 Amplitude equation reduction

We start with the generic stochastic equation (2.2) on the domain $[-L, L]$. For $\epsilon \ll 1$, the number of linearly unstable modes is given by the dimensionality of $\mathcal{N}$. We are interested in the dynamics of the dominant modes when the stable modes, $\hat{u}_k(t)\mathrm{e}_k$ for $\mathrm{e}_k \in \mathcal{N}^\perp$, are randomly forced. Here, $\mathcal{N}^\perp$ represents the subspace of fast modes orthogonal to $\mathcal{N}$. The noise term in Eq. (2.2) is therefore written as:

$$\xi(x,t) = \sum_{\mathrm{e}_k \in \mathcal{N}^\perp} q_k \dot{\beta}_k(t)\mathrm{e}_k(x). \tag{2.3}$$

The variable $\dot{\beta}_k(t)$ in the above equation corresponds to uncorrelated white noise, $\langle \dot{\beta}_m(t)\dot{\beta}_n(t')\rangle = \delta_{mn}\delta(t-t')$, and q_k represents the wave number dependence of the noise. Considering now the behaviour of small solutions at time scales of $O(\epsilon^{-2})$, we define $u(x,t) = \epsilon v(x, \epsilon^2 t)$ and use the scaling properties of the white noise to transform Eq. (2.2) to:

$$\partial_t v = \epsilon^{-2}\mathcal{L}v + \mathcal{J}v + \epsilon^{-1}\mathcal{B}(v,v) + \epsilon^{-1}\sigma\xi(x,t). \tag{2.4}$$

A detailed rigorous derivation of the pertinent amplitude equation for the dominant mode in the case where $\mathcal{J}$ is the identity operator can be found in Ref. [5]. We shall extend this

previous formalism here for the general case of $\mathcal{J}$ being any linear (differential) operator that commutes with $\mathcal{L}$, i.e. both operators have the same eigenfunctions, and for a finite dimensional kernel, i.e. $\dim(\mathcal{N}) = N_0$.

To obtain the amplitude equation for the dominant modes we consider a finite dimensional truncation of the above system and keep M fast modes in the series expansion, so that the total number of modes in the expansion is $N = N_0 + M$. We also consider Eq. (2.4) in a bounded domain, e.g. $[-\pi, \pi]$, and we project the field v onto $\mathcal{N}$ to get $v_1 = \mathcal{P}_c v$, where $\mathcal{P}_c$ is the corresponding projector to the null space, and onto its orthogonal subspace $\mathcal{N}^\perp$ to get $v_\perp = \mathcal{P}_s v$, where $\mathcal{P}_s = \mathcal{I} - \mathcal{P}_c$ with $\mathcal{I}$ being the identity operator. The resulting system of equations reads:

$$\partial_t v_1 = \mathcal{J} v_1 + 2\epsilon^{-1}\mathcal{P}_c\mathcal{B}(v_1, v_\perp) + \epsilon^{-1}\mathcal{P}_c\mathcal{B}(v_\perp, v_\perp), \tag{2.5 a}$$

$$\partial_t v_\perp = (\mathcal{J} + \epsilon^{-2}\mathcal{L})v_\perp + \epsilon^{-1}\mathcal{P}_s\mathcal{B}(v, v) + \epsilon^{-1}\sigma\xi(x, t). \tag{2.5 b}$$

By applying now techniques from homogenisation theory [38] and assuming the condition for the bilinear map of $\mathcal{P}_c\mathcal{B}(\mathrm{e}_k, \mathrm{e}_k) = 0$ for $k = 1, \ldots, N$, we can derive the homogenised (i.e. amplitude) equations that describe the dynamics of the unstable modes. The detailed derivation for a multidimensional null space is given in Appendix A.

In the case of 1D null space, we define the amplitude A for the dominant mode as $v_1 = A(t)\mathrm{e}_1$, and its corresponding equation is given by the SL equation with multiplicative noise (see Appendix A for details):

$$\dot{A} = (j_1 + \gamma_1\sigma^2)A - \gamma_2 A^3 + \sigma\sqrt{\gamma_a\sigma^2 + \gamma_m A^2}\,\dot{W}(t), \tag{2.6}$$

where $\dot{W}(t)$ is a white noise, and where the different coefficients are given in Eq. (A 21) from Appendix A. We therefore see that the coefficients explicitly depend on the nature

of the noise, i.e., the values of q_k, and the properties of the quadratic nonlinearity, which are dictated by $B_{n\ell k}$ given in Eq. (A 3).

In the case of a two-dimensional (2D) null space, the solution is expanded as $v_1 = a_1(t)\mathrm{e}_1 + a_2(t)\mathrm{e}_2$, and the coupled amplitude equations we obtain are of the form:

$$\dot{a}_1 = (j_1 + 2\gamma_1\sigma^2)a_1 - \gamma_2 a_1 A^2 + 2\sigma\sqrt{\gamma_a\sigma^2 + \gamma_m A^2}\,\dot{W}_1(t), \tag{2.7 a}$$

$$\dot{a}_2 = (j_1 + 2\gamma_1\sigma^2)a_2 - \gamma_2 a_2 A^2 + 2\sigma\sqrt{\gamma_a\sigma^2 + \gamma_m A^2}\,\dot{W}_2(t), \tag{2.7 b}$$

where we have defined the global amplitude $A(t) = \sqrt{a_1^2 + a_2^2}$, and the coefficients γ_1, γ_2, γ_a, and γ_m are given by Eqs. (A 21).

2.2 Analysis of the amplitude equation

The stationary statistical properties of the amplitude dynamics can be studied by solving the corresponding stationary Fokker-Planck equation. In the 1D case, the stationary probability density function (PDF) for the random variable A **in the Stratonovich interpretation** for natural boundary conditions is given by [16, 31]:

$$P(A) = \frac{N_c}{g(A)} \exp \int^A \frac{2r(z)}{g^2(z)} \mathrm{d}z, \tag{2.8}$$

where $r(A) = (j_1 + \gamma_1\sigma^2)A - \gamma_2 A^3$ and $g(A) = \sigma\sqrt{\gamma_a\sigma^2 + \gamma_m A^2}$, yielding in our case

$$P(A) = N_c(A^2 + \lambda^2\sigma^2)^{\alpha_1/2} \exp\left(-\mu A^2\right), \tag{2.9}$$

with:

$$\alpha_1(\sigma) = 2\frac{j_1 + (\gamma_1 + \gamma_2\lambda^2)\sigma^2}{\gamma_m\sigma^2} - 1, \quad \mu(\sigma) = \frac{\gamma_2}{\gamma_m\sigma^2}, \tag{2.10}$$

where we have defined the parameter $\lambda \equiv \gamma_a/\gamma_m$, and the normalisation constant N_c is given as $N_c = 2\mu^{\frac{\alpha_1+1}{2}}/\Gamma_\lambda(\alpha_1)$, where $\Gamma_\lambda(\alpha_1) = \int_{-\infty}^{\infty} x^{-1/2}(x+\mu\lambda^2\sigma^2)^{\alpha_1/2}\mathrm{e}^{-x}\,\mathrm{d}x$. It should be noted that the statistical properties of the fluctuating dominant mode depend on both the strength of the noise σ and the values of q_k (see §3 below for the example of the KS equation).

For a 2D null space, the stationary joint PDF for the two variables, $G(a_1, a_2)$, can also similarly be obtained by computing the corresponding stationary 2D Fokker-Planck equation. This yields to:

$$G(a_1, a_2) \propto (a_1^2 + a_2^2 + \lambda^2)^{\alpha_1'/2} \exp\left[-\mu'(a_1^2 + a_2^2)\right],$$

where the parameters α_1' and μ' are obtained from the expressions in Eq. (2.10) by replacing γ_1, γ_a, and γ_m with $2\gamma_1$, $4\gamma_a$, and $4\gamma_m$, respectively. The interesting point now is to study the behaviour of the PDF, $P(A)$, corresponding to the global amplitude $A = \sqrt{a_1^2 + a_2^2}$. To this end, we move to a polar coordinate system (A, θ) by applying the transformation $y_1 = A\sin\theta$ and $z_1 = A\cos\theta$, and we impose the normalisation condition between both distributions, $G(a_1, a_2)\mathrm{d}a_1\mathrm{d}a_2 = P(A, \theta)\mathrm{d}A\mathrm{d}\theta$, giving rise to a function of the form:

$$P(A) \propto A(A^2 + \lambda^2)^{\alpha_1'/2} \exp\left(-\mu' A^2\right). \tag{2.11}$$

Let us now apply the theory outlined above on a prototype model equation.

3 Case study: the noisy Kuramoto-Sivashinsky equation

Consider the noisy KS equation:

$$\partial_t u = -(\partial_x^2 + \nu\partial_x^4)u - u\partial_x u + \tilde{\sigma}\xi, \tag{3.1}$$

normalised to 2π-periodic domains so that $0 < \nu = (\pi/L)^2$, where $2L$ is the original length of the system. The equation corresponds to an important class of SES, active-dissipative nonlinear media, whose main features are the presence of mechanisms for instability/energy production at long scales ($\partial_x^2 u$) and stability/energy dissipation at short scales ($\partial_x^4 u$). Both without and with the noise term, the KS equation has attracted a lot of attention since it appears in a wide variety of applications and physical phenomena. These include instabilities of flame fronts, models of collisional trapped ion modes in plasmas, dissipative turbulence, interfacial instabilities in two-phase flows, reaction-diffusion systems, the control of surface roughness in the growth of thin solid films by sputtering, step dynamics in epitaxy, the growth of amorphous films, and models in population dynamics [9, 11, 24, 25, 35, 48, 50]. A detailed derivation of the noisy KS equation in the context of thin-film hydrodynamics is given in Appendix B.

The KS equation represents an ideal candidate for our studies due to the extensive rigorous and computational results available. It is often used as a paradigmatic partial differential equation (PDE) that has low dimensional behaviour producing complex dynamics such as chaos - [19, 20, 22, 36, 49, 53, 54]. The existence and uniqueness of solutions for the stochastic KS equation have been proven in [10]. The effect of weak additive white noise on transitions between stable fixed-point solutions and stable travelling-wave solutions of the KS equation has been considered numerically in [51] and the relationship between noise-induced transitions and the underlying attractors are explored.

By assuming $\nu = 1 - \epsilon^2$ and $\tilde{\sigma} = \epsilon\sigma$, Eq. (3.1) is rewritten as:

$$\partial_t u = -(\partial_x^2 + \partial_x^4)u + \epsilon^2 \partial_x^4 u - u\partial_x u + \epsilon\sigma\xi. \tag{3.2}$$

We can therefore read off all the different terms in Eq. (2.2) as $\mathcal{L} = -\partial_x^2 - \partial_x^4$, $\mathcal{J} = \partial_x^4$, and $\mathcal{B}(u,u) = -u\partial_x u$. It is important to emphasise that in this setting, the term $\epsilon^2\partial_x^4 u$ represents a linear instability term that can destabilize the dominant modes of the equation. Note that it is controlled by the parameter ϵ^2 which measures the distance from bifurcation. In this sense, a decrease in $\nu = 1-\epsilon^2$ below the bifurcation point $\nu = 1$ (and hence increasing $\epsilon > 0$) reduces the linearly stabilizing term $\partial_x^4 u$ and therefore destabilizes the dominant modes[3]. In our analysis we assume solutions of zero mean and we shall consider both the case of Dirichlet boundary conditions (DBC), i.e. $u(-\pi,t) = u(\pi,t) = 0$, and periodic boundary conditions (PBC), **together with the additional condition that the derivatives of u are also periodic. In the case of DBC we also consider an initial condition given as an odd periodic small function, e.g.** $u(x,0) = \epsilon\sin(kx)$, and the null space of $\mathcal{L}$ is 1D:

$$\mathcal{N}(\mathcal{L}) = \text{span}\left\{\sin(\cdot)\right\},$$

and the solution can be expanded in the basis $\{\mathrm{e}_k(x) = c_k\sin(kqx)\}$, where $q = \pi/L = 1$ and c_k's are normalisation constants. On the other hand, for PBC the null space of $\mathcal{L}$ is 2D:

$$\mathcal{N}(\mathcal{L}) = \text{span}\left\{\sin(\cdot),\, \cos(\cdot)\right\},$$

and the solution is expanded in the exponential Fourier basis $\{\mathrm{e}_{2k-1} = c_{2k-1}\sin(kqx)$, $\mathrm{e}_{2k} = c_{2k}\cos(kqx)\}$ for $k = 1, 2, \ldots$. By applying the multiscale formalism developed in

[3] Note that when the KS equation is written in this form, multiscale analysis can be used in order to obtain the amplitude equation in a rigorous and systematic way. See Appendix A for details.

§2.1, we then obtain that the amplitude equation for the dominant mode is given either by Eq. (2.6) for DBC or by Eqs. (2.7) for PBC, with $j_1 = 1$ and the following coefficients:

$$\gamma_1 = -\frac{3}{8}\frac{q_2^2}{\lambda_2(\lambda_2+\lambda_3)} + \frac{1}{8}\sum_{n=3}^{N}\frac{q_n^2}{\lambda_n}\left(\frac{n-1}{\lambda_n+\lambda_{n-1}} - \frac{n+1}{\lambda_n+\lambda_{n+1}}\right), \tag{3.3 a}$$

$$\gamma_2 = \frac{1}{48}, \qquad \gamma_m = \frac{q_2^2}{576}, \tag{3.3 b}$$

$$\gamma_a = \frac{1}{8}\frac{q_2^2 q_3^2}{\lambda_3(\lambda_2+\lambda_3)^2} + \frac{1}{8}\sum_{n=3}^{N} q_n^2\left(\frac{q_{n+1}^2}{\lambda_{n+1}(\lambda_n+\lambda_{n+1})^2} + \frac{q_{n-1}^2}{\lambda_{n-1}(\lambda_n+\lambda_{n-1})^2}\right), \tag{3.3 c}$$

where $\lambda_k = k^4 - k^2$, and the noise in the amplitude equation is interpreted in the Stratonovich sense (see Appendix A). From the above expressions it is interesting to note that several situations arise for different cases of noise. For example, for a highly degenerate noise acting on the first stable mode only (Case I, $q_k = \delta_{k,2}$), there is only multiplicative noise ($\gamma_a = 0$). On the other hand, when the noise acts on both the second and third mode (Case II, $q_k = \delta_{k,2} + \delta_{k,3}$), the multiplicative noise is corrected by an additive-like term ($\gamma_a \neq 0$). Finally, when the noise acts on the third mode only (Case III, $q_k = \delta_{k,3}$), the resulting amplitude equation contains no noise ($\gamma_m = \gamma_a = 0$). **It is worth mentioning that in the case of a thin film flowing down an uneven wall (see Appendix B), forcing the KS equation with a highly degenerate noise would correspond to randomly vibrated substrates with sinusoidal shape, and hence substrates with a specific selected wavenumber, for example the second one (which would correspond to Case I) or the third one (Case III).**

In the following, we analyse analytically and numerically the dynamics of the amplitude of the dominant mode $A(t)$ by considering the above three different cases of noise separately. To solve numerically the KS equation we adopt a pseudo-spectral method for

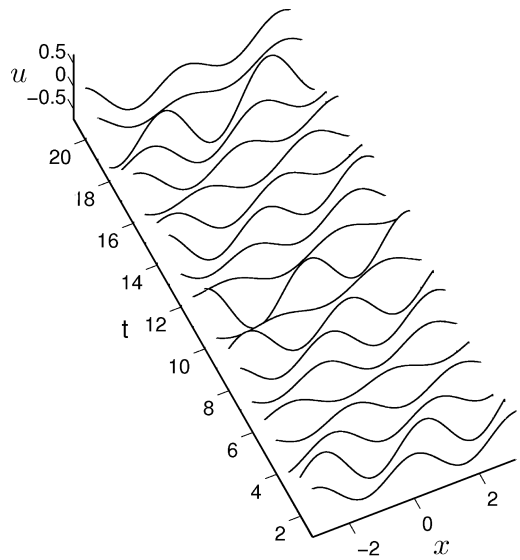

FIGURE 1. Typical spatio-temporal evolution of the noisy KS equation (3.1) with PBC for $\sigma = 10$ and $\epsilon = 0.025$, and imposing a highly degenerate noise acting on the first stable mode (Case I).

the spatial derivatives that uses the Fast Fourier Transform (FFT) to transform the solution to Fourier space. The nonlinear terms are evaluated in real space and transformed back to Fourier space by using the inverse FFT. The solution is then propagated in time by making use of a fourth-order Runge-Kutta scheme. In our simulations we have chosen a time step of $\Delta t = 0.1$, and the numerical error has been controlled by monitoring some constant quantity, namely the spatially averaged solution $\langle u \rangle = \frac{1}{2L}\int_{-L}^{L} u(x,t)\mathrm{d}x$, so that with the chosen time step it remains constant during all the numerical experiments.

3.1 Case I. Amplitude equation with multiplicative noise: Noise induced critical state transitions

We start by considering the case of highly degenerate noise acting on the first stable mode only so that the resulting amplitude equation for the dominant mode contains a pure multiplicative noise term ($\gamma_a = 0$). Typical snapshots of the spatio-temporal evolution of the KS Eq. (3.1) in this noise setting and subject to PBC with $\sigma = 10$ and $\epsilon = 0.025$ are depicted in Fig. 1. The interesting point here is that as a consequence of the multiplicative noise in the amplitude equation, several state transitions may arise depending on the value of the noise strength. As was pointed out in [31], the presence of multiplicative noise, and in particular the fact that the coefficient $\sigma\sqrt{\gamma_m}A$ from Eq. (2.6) vanishes at $A = 0$, becomes crucial for the description of the asymptotic stability of the stationary PDF in terms of Lyapunov functions, giving rise then to different scenarios depending on the integrability of the PDF, i.e. whether the PDF can be normalised or not. As we shall show now, different states can be observed by simply changing the strength of the noise. The results are presented separately for each case of boundary conditions.

In the case of DBC, the PDF of the dominant mode amplitude, $A(t) = \hat{u}_1(t)$, is given by Eq. (2.9) with $\lambda = 0$. In this case there exist different states for the fluctuating amplitude that can be characterised by looking both at the maximum location and integrability of the amplitude PDF [16, 31]. First, we observe that as long as $\alpha_1 > 0$ the maximum of $P(A)$ occurs at a finite value, $A_{\max} > 0$, and then the state of A is characterised by finite fluctuations around a mean value (state I). On the other hand, for $-1 < \alpha_1 \leq 0$,

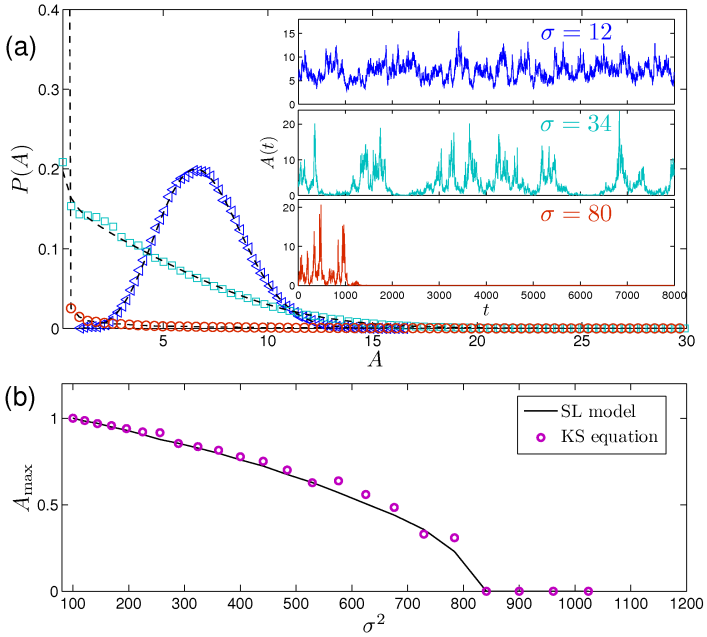

FIGURE 2. (Colour online) Numerical results for the noisy KS equation (3.1) integrated on a $[-\pi, \pi]$ domain with DBC (1D null space). (a) PDF of the first-mode amplitude calculated for $\sigma = 12$, $\sigma = 34$, and $\sigma = 80$, with $\epsilon = 0.05$. Dashed lines correspond to a data fit to a function of the form given by Eq. (2.9) with $\lambda = 0$. The inset shows the typical fluctuations of the amplitude at each of the three values of σ. (b) Maximum location of the amplitude PDF at different values of σ. The solid line corresponds to the numerical solution of the SL model. All values have been normalised to the corresponding value at $\sigma = 10$.

the maximum is located at zero, $A_{\max} = 0$, and the amplitude fluctuates intermittently between zero and a finite value (state II, see also below in §3.1.1 for a detailed statistical analysis of this state). These two states are separated by the critical value:

$$\sigma_{\mathrm{I}} = (\gamma_m/2 - \gamma_1)^{-1/2}. \tag{3.4}$$

Note that for $\gamma_1 > 0$, this transition can only be observed as long as $\gamma_m > 2\gamma_1$, while it is always observed for $\gamma_1 < 0$. By computing the maximum of $P(A)$ at different values

of σ we can then characterise the critical behaviour as: $A_{\max} = |\sigma_{\rm I}^2 - \sigma^2|^{1/2}/(\sigma_{\rm I}\sqrt{\gamma_2})$ for $\sigma \leq \sigma_{\rm I}$, and $A_{\max} = 0$ otherwise, so that $A_{\max}$ and σ^2 are the order and control parameter, respectively, describing the critical transition. By using now the particular values obtained for the KS equation [from Eq. (3.3) we get $\gamma_1 = -1/2688$, $\gamma_2 = 1/48$, and $\gamma_m = 1/576$] we find $\sigma_{\rm I} = 28.3$ in excellent agreement with the numerical results (presented in Fig. 2, where we obtain $\sigma_{\rm I} \simeq 29$). Finally, we note that since $\gamma_1 < 0$, a second transition occurs when $\alpha_1 \leq -1$. In this situation, it is not possible to define Lyapunov functions to show the existence of a globally stable stationary PDF for A which can be normalised [31]. As a consequence, the PDF converges to a Dirac delta function, $P(A) = \delta(A)$, describing then a completely stabilised state with $A = 0$ (state III). The critical value $\sigma_{\rm II}$ for this second transition corresponds to:

$$\sigma_{\rm II} = \sqrt{1/|\gamma_1|}, \tag{3.5}$$

which for the KS equation gives $\sigma_{\rm II} = 51.8$, in very good agreement with the numerical results [see the bottom panel in the inlet of Fig. 2(a)]. Interestingly, **such stabilisation effect is reflected on the time averaged solution $\langle u(x,t)\rangle_t$ [see solid line in Fig. 3(b)]: since the dominant mode has been completely stabilised, the dynamics of the solution is only affected by the noise coming from the stable modes, which is wiped out after time averaging, obtaining therefore a zero spatial solution, i.e. $\langle u(x,t)\rangle_t = 0$.** This is in contrast to the inhomogeneous solution observed for smaller values of σ corresponding to state I [see solid line in Fig. 3(a)].

When we consider the case of PBC, the amplitude PDF is given by

$$P(A) \propto A^{\alpha_2} \exp\left(-\mu' A^2\right), \tag{3.6}$$

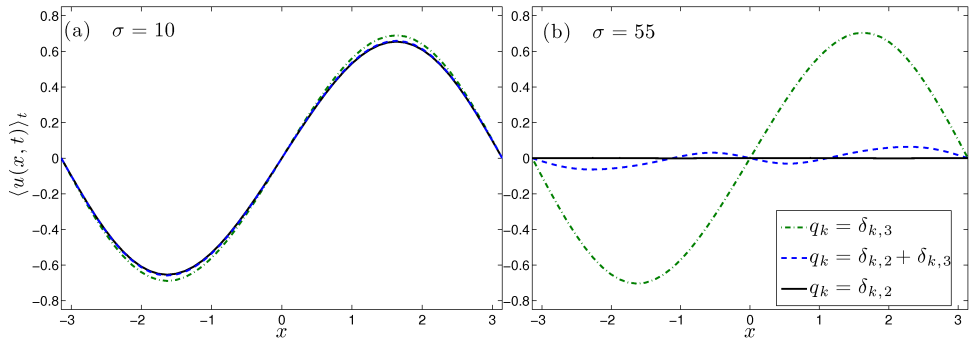

FIGURE 3. (Colour online) Time averaged solution of the noisy KS equation solved with DBC for $\epsilon = 0.1$ and $\sigma = 10$ (a) and 55 (b) for the case of: highly degenerate noise acting on the second mode (case I, solid line), degenerate noise acting on both the second and third mode (case II, dashed line), and highly degenerate noise acting on the third mode (case III, dot-dashed line).

where now $\alpha_2 = (1+2\gamma_1\sigma^2)/(2\gamma_m\sigma^2)$ and $\mu' = \gamma_2/4\gamma_m$. We first note that the transitions between different states can only occur if and only if $\gamma_1 < 0$. In such a case, the critical values for the first and second transitions are found to be:

$$\sigma_{\rm I} = \sqrt{1/2|\gamma_1|}, \qquad \sigma_{\rm II} = [2(|\gamma_1| - \gamma_m)]^{-1/2}. \tag{3.7}$$

Noteworthy is that the second transition can only occur as long as $\gamma_m < |\gamma_1|$. Otherwise, the completely stabilised state III is never observed, and the PDF tends to $P(A) \sim A^{\alpha_\infty}$ as $\sigma \to \infty$, with $\alpha_\infty = -|\gamma_1|/\gamma_m$. By using the KS coefficients given in Eqs. (3.3), we obtain the first transition to occur at $\sigma_{\rm I} = 36.3$, in excellent agreement with the numerical results presented in Fig. 4. The second transition, however, cannot be observed since the condition $\gamma_m < |\gamma_1|$ does not hold, giving an asymptotic behaviour with $\alpha_\infty = -0.21$, again in very good agreement with the numerical data [cf. Fig. 4(b)].

It is important to remark that the reason why we observe such large values

of σ for which the different transitions occur (see e.g. Fig. 2 with $\sigma = 12, 34, 80$) is a consequence of the scaling of the noise we used in Eq. (2.2). The actual noise we are considering is $\mathcal{O}(\epsilon\sigma)$, leading therefore to values which are much smaller, namely $0.6, 1.7$, and 4, respectively, for the noise strength used in Fig. 2. Let us also emphasize that strictly speaking, such scaled perturbations are still beyond the region of validity of the asymptotic analysis, $\epsilon \to 0$ for fixed σ, i.e. $\epsilon\sigma = 4 > 1$. Nevertheless, we have performed extensive numerical computations by choosing different values of ϵ ranging in $\epsilon \in [0.02, 0.1]$, observing the same results in all the cases, which then points to the robustness of the perturbation scheme. This also indicates that our numerical results are consistent with the asymptotic analysis presented in §2.1.

3.1.1 *Universal intermittent behaviour*

Let us focus here on the intermittent behaviour observed between the two transitions, $\sigma_{\rm I} < \sigma < \sigma_{\rm II}$, for DBC. It is worth emphasising at this point that on-off intermittency is a crucial universal feature of many nonlinear systems close to criticality, and reflects a transition from order/coherence to a disordered state (hence understanding the statistical properties of intermittency is crucial for the characterisation of this transition). In our case, it reflects the transition between an initially inhomogeneous state in space to a final zero state (see solid line in Fig. 3).

Figure 5 depicts the dynamics of the amplitude calculated by using $\sigma = 48$, which for DBC is close to the second critical transition $\sigma_{\rm II}$. In this regime, fluctuations are clearly dominated by an on-off intermittent, or burst-like behaviour. As was pointed out

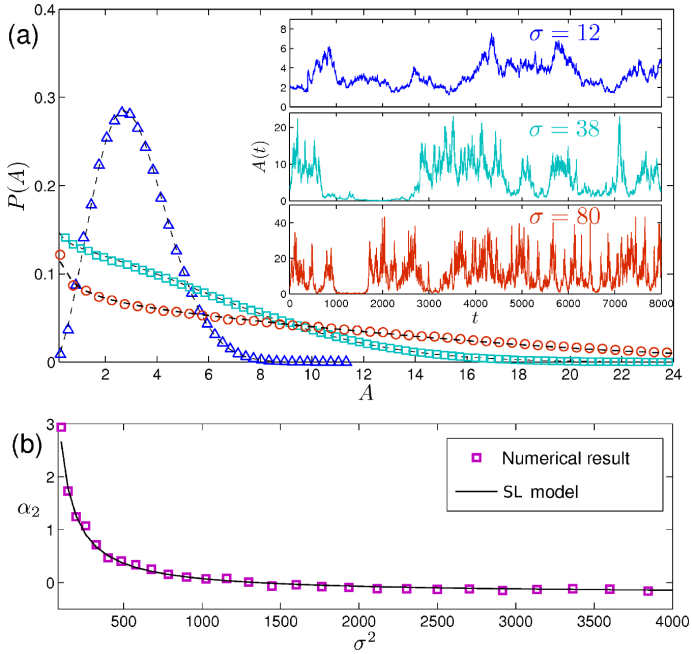

FIGURE 4. (Colour online) Numerical results for the noisy KS equation (3.1) integrated on a $[-\pi, \pi]$ domain with PBC (2D null space). (a) PDF of the first-mode amplitude calculated for $\sigma = 12$, $\sigma = 38$, and $\sigma = 80$, with $\epsilon = 0.025$. Dashed lines correspond to a data fit to a function of the form given by Eq. (3.6). The inset shows the typical fluctuations of the amplitude at each of the three values of σ. (b) Exponent α_2 obtained from the data fit at different values of σ. The solid line corresponds to the analytical solution of the SL model given by Eq. (3.6).

in Refs. [15, 39], such kind of on-off intermittency can be characterised by studying the statistical properties of the waiting time between two consecutive bursts, defined as large fluctuations above a given small threshold, $A > c_{\rm th}$. Given the SL amplitude equation (2.6), we can obtain an analytic expression for the PDF of the waiting times, $P(T)$, as follows.

Let us assume an initial value which is below the threshold, i.e., $A_i \equiv A(t = 0) < c_{\rm th}$. We then seek the probability $P(T)$ that at time T, the variable A reaches the threshold

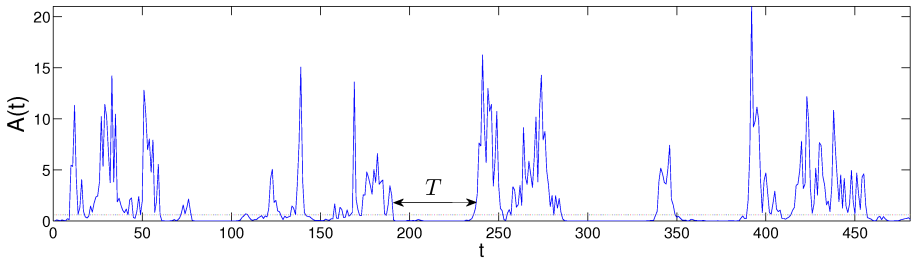

FIGURE 5. (Colour online) Time evolution of the dominant mode amplitude $A(t)$ for DBC with $\sigma = 48$. The waiting time between two consecutive large events is denoted as T. The dashed line represents the position of the chosen threshold $c_{\rm th}$ which defines the zero state as $A \leq c_{\rm th}$.

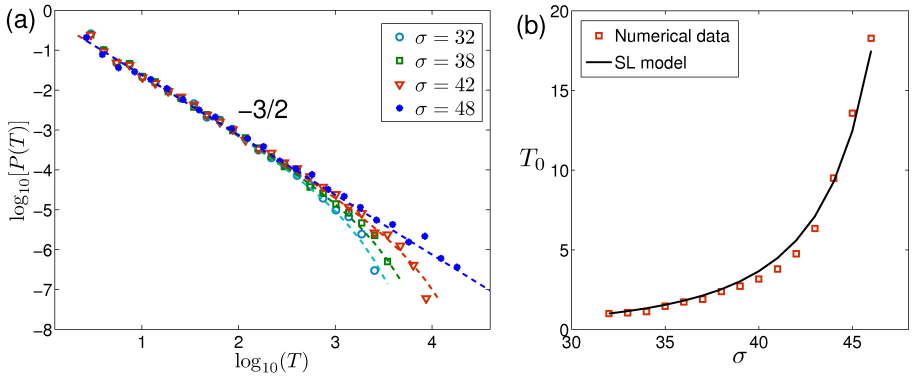

FIGURE 6. (Colour online) Statistical analysis of the waiting times between two consecutive bursts observed in the intermittent state II for DBC. (a) PDF of the waiting times calculated by using different noise strengths. The dashed line corresponds to a data fit to $P(T) = NT^{-\tau}\exp(-T/T_0)$ with $\tau = 1.5$. The value of the threshold used to define the waiting times T is $c_{\rm th} = 1$. (b) Value of the fitted time scale T_0 as a function of σ. The solid line corresponds to the analytical expression given in Eq. (3.9). All values have been normalised to the corresponding value at $\sigma = 12$.

$c_{\rm th}$ for the first time. In this close-to-zero state, the amplitude is found numerically to be $A \lesssim 0.1$, and therefore small enough to neglect the nonlinear term in the SL equation. More precisely, we first introduce the transformation $y = \log A$, and assume that $y \ll 0$

to obtain the following linearised equation:

$$\dot{y} = \kappa + \sigma\sqrt{\gamma_m}\,\dot{W}(t), \tag{3.8}$$

defined in the semi-infinite domain $y \in (-\infty, y_0]$ with adsorbing boundary conditions at the origin $y_0 \equiv \log c_{\rm th}$, and where $\kappa = 1 + \gamma_1\sigma^2$. We note that the choice of an adsorbing boundary condition at the origin is required to ensure that the variable A leaves the domain once it reaches the threshold. The problem now reduces to finding the probability that at time T the new variable y reaches the origin for the first time. This corresponds to the well-known "first-passage probability" (FPP) of the random walk in semi-infinite domains (see Ref. [43]), which simply reduces to solving the Fokker-Planck equation for the probability $p(y,t)$:

$$\partial_t p(y,t) = -\kappa\partial_y p(y,t) + \gamma_m\sigma^2\frac{1}{2}\partial_y^2 p(y,t).$$

This can readily be done by using the method of images, obtaining:

$$p(y,t;y_i,0) = \frac{1}{\sqrt{\pi 4\gamma_m\sigma^2 t}}[\mathrm{e}^{-(y-y_i+\kappa t)^2/4\gamma_m\sigma^2 t} - \mathrm{e}^{\kappa y_i/(\gamma_3\sigma)^2}\mathrm{e}^{-(y+y_i+\kappa t)^2/4\gamma_m\sigma^2 t}],$$

where $y_i = \log A_i$ is the initial value and we have assumed without loss of generality that $c_{\rm th} = 1$, and therefore $y_0 = 0$. The FPP can now be obtained as:

$$P(T) = -\int_{-\infty}^{0} \partial_t p(y,t;y_i,0)|_{t=T}\,\mathrm{d}y,$$

from which we get:

$$P(T) = \frac{-y_i}{\sqrt{\pi 4\gamma_m\sigma^2 T^3}}\mathrm{e}^{-(-y_i+\kappa T)^2/4\gamma_m\sigma^2 T}.$$

In the long-time limit $T \to \infty$, the above expression becomes:

$$P(T) \approx T^{-3/2}\mathrm{e}^{-T/T_0}, \tag{3.9}$$

with a time scale $T_0 = [2\sigma\sqrt{\gamma_m}/(1+\gamma_1\sigma^2)]^2$. Therefore, at the critical point $\sigma = \sigma_{\rm II}$ the above PDF becomes a pure power-law dictated by a universal exponent 3/2 that does not depend on the particular model we are using, i.e., it does not depend on the coefficients of the SL equation. The numerical results obtained with the KS equation are presented in Fig. 6 where we can see an excellent agreement with the above expression. It should be noted that far from the critical point ($\sigma < \sigma_{\rm II}$), the power-law is exponentially corrected with the time scale T_0 [cf. Fig. 6(b)].

3.2 Case II. Amplitude equation with both additive and multiplicative noise

Let us now consider the noise term acting on both the second and third mode, i.e. $q_k = \delta_{k,2} + \delta_{k,3}$ with DBC. In this setting, the amplitude equation is given by Eq. (2.6) with both γ_a and γ_m being different from zero. Although the noise is still highly degenerate, it induces the same effect as when we consider the noise acting on the whole subspace of stable modes, i.e., $q_k = 1$ for $k \geq 2$ (and therefore having space-time white noise). For simplicity, we shall therefore restrict our analysis to the case with only the third and second modes being stochastically forced.

First, we note that in this case of noise we can still identify two different dynamic behaviours (states) for the dominant amplitude. At low values of σ we have that, as it occurred in case I, the location of the maximum of $P(A)$ is found to be at a finite value, $A_{\rm max} > 0$, and the dominant mode fluctuates around a finite mean value. As the noise strength is increased, the maximum location approaches zero and the first mode component $\hat{u}_1$ may reach zero. Computing the maximum location by considering the PDF given by Eq. (2.6) we obtain that the critical value, $\sigma_{\rm I}$, separating these two states

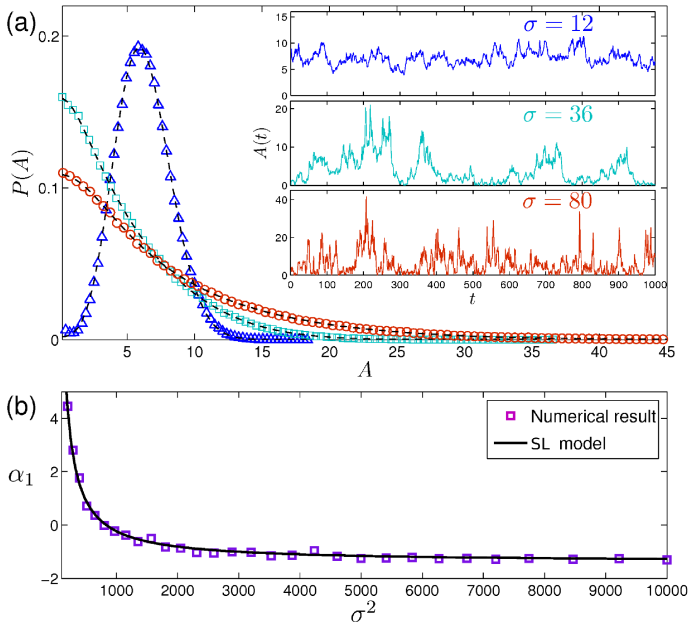

FIGURE 7. (Colour online) Numerical results for the noisy KS equation (3.1) integrated on a $[-\pi, \pi]$ domain with DBC and with a noise acting on the second and third stable modes (case II). (a) PDF of the first-mode amplitude calculated for $\sigma = 12$, $\sigma = 36$, and $\sigma = 80$, with $\epsilon = 0.1$. The inset shows the typical fluctuations of the amplitude at each of the three values of σ. (b) Exponent α_1 obtained from the PDF at different values of σ. The solid line corresponds to the analytical solution of the SL model given by Eq. (2.10).

corresponds to the same value as in case I of noise given by Eq. (3.4). In this situation, however, the presence of the additive noise keeps the first mode from remaining at the zero position, and hence ruling out the intermittent dynamics observed in the previous section. Further, as the noise strength is increased, the PDF can now be always normalised so that the completely stabilised state III is never observed.

Figure 7 depicts typical numerical results for the KS equation. The coefficients of the SL equation in this case are $\gamma_1 = -1/2688 + 1/52416$, $\gamma_2 = 1/48$, $\gamma_a = 1/580608$, and $\gamma_m = 1/576$, so that we have $\sigma_{\mathrm{I}} \simeq 28.6$. To compare with the results presented in § 3.1,

we compute the amplitude of the dominant mode by taking the absolute value of the first mode, i.e. $A(t) = |\hat{u}_1(t)|$, for different strengths of the noise. The PDFs of A for $\sigma = 12$, 36 and 80 are presented in Fig. 7(a). We can see that the presence of the extra term controlled by γ_a in the amplitude equation keeps the dominant mode away from zero and hence of being completely stabilised. As before, we find excellent agreement between the numerical results and the analytical derivation given by Eq. (2.6). Indeed, Fig. 7(b) shows a comparison of the numerical value of the exponent α_1 obtained from a data fit of the PDF with the analytical value given by Eq. (2.10) for different strength of the noise. Moreover, by computing the time average of the spatio-temporal solution we can see that at low values of the noise strength ($\sigma = 10$), the averaged solution still retains the sinusoidal shape [see dashed line in Fig. 1(a)], corresponding to the first state where $A_{\max} > 0$. At higher noise strength values ($\sigma = 55$), however, the averaged solution losses the sinusoidal shape [see dashed line in Fig. 1(b)], corresponding to the second state with $A_{\max} = 0$. In contrast to the stabilised state observed in case I of noise, the averaged solution remains now noisy since the dominant mode is never completely stabilised.

3.3 Case III. Amplitude equation without noise

Finally, we consider the case of DBC with a noise acting only on the third mode ($q_k = \delta_{3k}$). In this setting, both noise coefficients are zero ($\gamma_m = \gamma_a = 0$) with a positive coefficient $\gamma_1 > 0$ for any value of the disorder strength. As a result, the dynamics of the dominant mode is not affected by the noise, and only its steady state A_{st}, given by the

stationary solution of the deterministic SL Eq. (2.6) as:

$$A_{st} = \sqrt{\frac{1+\gamma_1\sigma^2}{\gamma_2}}, \tag{3.10}$$

will be affected for sufficiently large σ. When we apply this noise setting to the KS equation we obtain $\gamma_1 = 1/52416$, so that only for values of noise strength as large as $\sigma \sim 230$ such effect will start to be relevant. As we see in Fig. 3 (see dot-dashed line), the time averaged solution $\langle u(x,t)\rangle$ is not affected when the noise is increased up to $\sigma = 55$. It is also worth emphasising that we would obtain the same result had we considered a noise acting on all the stable odd modes. It means that this kind of noise acting on the odd modes only is filtered out by the quadratic nonlinearity interaction, such that it has no effect on the dominant mode dynamics.

4 Numerical results in a regime beyond the instability onset

Let us consider now the situation where there are more than one unstable modes. Clearly, the theory presented in §2.1 is not expected to be valid in this case. We shall therefore numerically integrate the noisy KS equation by taking $\epsilon = 0.87$ such that the number of unstable modes is two. We are interested to see whether stabilisation phenomena as presented in §3.1 for noise case I can still be observed by appropriately tuning the noise. To this end we choose the noise so that it acts on the first stable mode, corresponding to taking $q_k = \delta_{k,3}$, and we study the dynamics of the amplitude of both the first ($A_1(t) = |\hat{u}_1(t)|$) and second ($A_2(t) = |\hat{u}_2(t)|$) modes.

The corresponding numerical results are presented in Fig. 8. Noteworthy is that both modes can be completely stabilised as the noise strength is increased up to values of

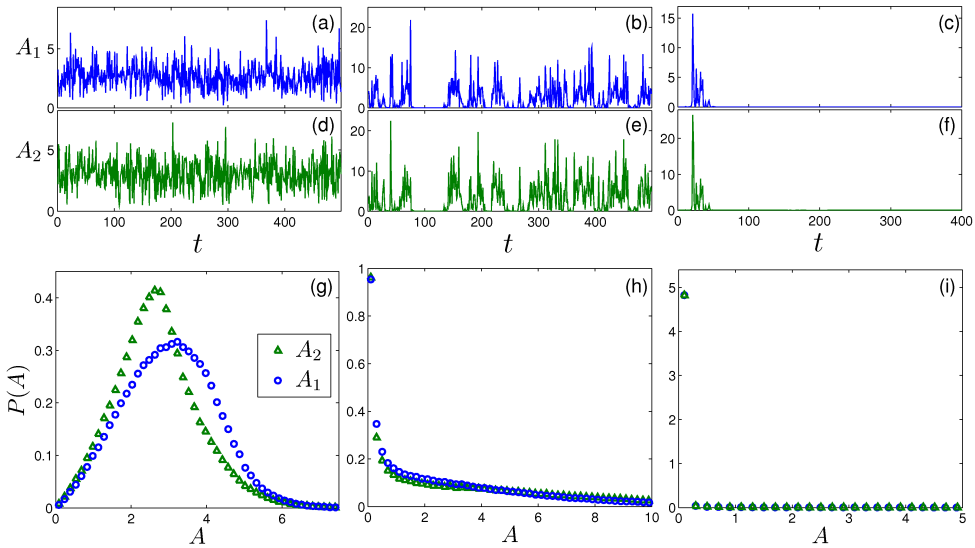

FIGURE 8. (Colour online) Numerical results for the noisy KS equation (3.1) integrated on a $[-\pi, \pi]$ domain in a regime far from the stability onset ($\epsilon = 0.87$) with a highly degenerate noise acting on the first stable mode. Panels (a), (b), and (c) show the time signal of the amplitude of the first dominant mode $A_1(t)$ for $\sigma = 40$, 230 and 270, respectively. Panels (d), (e), and (f), show the corresponding time series of the second unstable mode $A_2(t)$ for the same noise strengths. Bottom panels (g), (h), and (i) show the PDF of each mode for the three different values of σ.

$\sigma \sim 270$, going through the same critical transitions as in §3.1. As before, we perform a statistical analysis of the waiting times between two consecutive bursts which are observed in the intermittent state corresponding to $\sigma = 260$. The results for both modes are presented in Fig. 9, where we observe that the PDF of the waiting times for both modes is dominated by a heavy-tail function with an exponent 3/2. Therefore, our results show that even in situations relatively far from the instability onset, we can still observe stabilisation and critical transition induced by pure additive noise. We note, however,

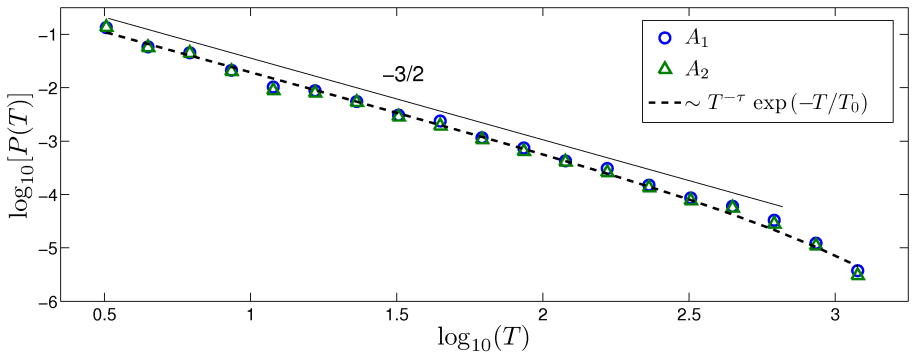

FIGURE 9. (Colour online) PDF of the waiting times between two consecutive bursts obtained from the time series of the two dominant modes A_1 and A_2 for $\sigma = 260$. The dashed line corresponds to a data fit to $P(T) = NT^{-\tau}\exp(-T/T_0)$, with $\tau = 1.5$.

that the noise strength needs to be much larger now (up to $\sigma = 270$) to completely stabilise the dominant modes.

5 Conclusions

We have undertaken an analytical and numerical study on the effect of additive noise on active nonlinear SES. For simplicity we have focused on SES with quadratic nonlinearities, in particular the KS equation, and randomly perturbed in the vicinity of a primary bifurcation point, where the dynamics is described by a single unstable dominant mode.

By adding a stochastic forcing acting on the first stable mode, we have been able to provide a detailed and systematic investigation of the transitions between different states. In particular, we have observed that at low values of the noise strength, the amplitude of the dominant mode is dominated by finite fluctuations around the zero–noise solution ($\sigma = 0$). On the other hand, at high values of the noise strength the dominant mode can be completely stabilised, yielding the zero solution when the spatio-temporal evolution

of the system is time averaged. These two states are continuously connected by another intermediate state where the solution intermittently fluctuates between the first non-zero state and the final zero state, and it is characterised by a burst-like dynamics. The transitions between the different states have been completely characterised through critical exponents, obtaining excellent agreement between theory and numerical results. In addition, we have been able to rigorously derive the critical exponent 3/2 describing the waiting times of the intermittent state II. It is important to emphasise that the derivation has been done for general SES whose dominant mode amplitude is given by Eq. (2.6). In this sense, the exponent 3/2 reveals the existence of an underlying universal mechanism dictated by the random walk properties. Interestingly, the same exponent has been ubiquitously found in many physical systems that display avalanche or burst-like dynamics. Examples include neuronal avalanches in the spontaneous cortex activity [47], on-off intermittency in electroconvection of nematic liquid crystals [21], or interface dynamics in disordered media [28, 40].

When the noise acts on the whole subspace of stable modes (or equivalently on the first and second stable modes) the dynamics of the dominant mode is corrected by an additive noise which keeps the system away of being completely stabilised, with the loss of any critical intermittent behaviour. Again, the numerical results in this situation are found to be in very good agreement with the analytical predictions. We have also considered a case where the noise acts on the second stable mode only (or equivalently on the stable odd modes). In this situation the quadratic nonlinearity can filter out the noise such that the dynamics of the dominant mode is not affected by the stochastic forcing applied to the system.

It is important to remark that, although the theory presented in this work has been applied to the KS equation, our analysis is rather general and could be easily extended to other models, such as the stochastic Burgers equation [4, 44] , used for example as a prototype for 1D turbulence albeit without pressure gradient, the Kardar-Parisi-Zhang (KPZ) equation, largely studied in the context of surface growth [1], or the stochastic Swift-Hohenberg equation, often used as a model for Rayleigh-Bénard convection, which in turn is commonly used as a prototype to study instabilities out of equilibrium in SES [7]. It should also be noted that the approach followed in this study is very robust: The stochastic SL equation (2.6) is the universal amplitude equation for SPDEs with quadratic nonlinearities, as proved in Ref. [5]. Furthermore, the characterisation of the different regimes depending on the strength of the noise, and in particular the calculation of the critical exponent that describes the intermittent behaviour are systematic and rigorous. It is expected that the techniques and methodologies developed in this study can be extended to more general classes of problems, where noise induced phenomena occur.

Finally, by performing numerical integrations of the noisy KS equation in a regime relatively far from the instability onset, where there are two unstable dominant modes, we have observed similar stabilisation and state transitions induced by an additive noise which is acting on the first stable mode only. It is important to remark that, although there is no theory in this case, our numerical study provides evidence that such stabilisation and noise induced state transitions are not restricted to a regime close to the instability onset.

Appendix A Derivation of the amplitude equation

We use techniques from homogenisation theory [38] and singular perturbation theory for Markov processes [37] (see also [32]) to derive the amplitude equation that describes the dynamics of Eq. (2.4) near the bifurcation point.

We consider a finite-dimensional truncation of Eqs. (2.5) up to N modes with a finite-dimensional null space, i.e. $\dim(\mathcal{N}) = N_0$, so that the number of fast modes is $M = N - N_0$. The kernel $\mathcal{N}$ of $\mathcal{L}$ is then spanned by the first N_0 eigenfunctions, and we can write:

$$v_1 = \sum_{k=1}^{N_0} a_k \mathrm{e}_k \quad \text{and} \quad v_\perp = \sum_{k=N_0+1}^{N} y_k \mathrm{e}_k,$$

which when introduced into Eqs. (2.5) yields the following system of equations:

$$\dot{a}_m = \frac{1}{\epsilon} f_0^m(\boldsymbol{a}, \boldsymbol{y}) + f_1^m(\boldsymbol{a}), \quad m = 1, \dots N_0, \tag{A 1 a}$$

$$\dot{y}_k = -\frac{1}{\epsilon^2}\lambda_k y_k + \frac{1}{\epsilon} g_0^k(\boldsymbol{a}, \boldsymbol{y}) + g_1^k(\boldsymbol{y}) + \frac{1}{\epsilon}\sigma q_k \dot{\beta}_k, \quad k = N_0 + 1, \dots N \tag{A 1 b}$$

where $\boldsymbol{a} = (a_1, \dots, a_{N_0})^T$ and $\boldsymbol{y} = (y_{N_0+1}, \dots, y_N)^T$. The different vector field terms in the above system of equations are given as:

$$f_0^m(\boldsymbol{a}, \boldsymbol{y}) = 2\sum_{n=1}^{N_0} a_n \sum_{\ell=N_0+1}^{N} B_{n\ell m} y_\ell + \sum_{n,\ell=N_0+1}^{N} B_{n\ell m} y_n y_\ell, \tag{A 2 a}$$

$$g_0^k(\boldsymbol{a}, \boldsymbol{y}) = \sum_{n,\ell=1}^{N_0} B_{n\ell k} a_n a_\ell + 2\sum_{n=1}^{N_0} a_n \sum_{\ell=N_0+1}^{N} B_{n\ell k} y_\ell + \sum_{n,\ell=N_0+1}^{N} B_{n\ell k} y_n y_\ell, \tag{A 2 b}$$

$$f_1^m(\boldsymbol{a}) = j_m a_m, \qquad g_1^k(\boldsymbol{y}) = j_k y_k, \tag{A 2 c}$$

where the coefficients j_k and λ_k are defined as $\mathcal{J}\mathrm{e}_k = j_k \mathrm{e}_k$, and $-\mathcal{L}\mathrm{e}_k = \lambda_k \mathrm{e}_k$, respectively, and

$$B_{n\ell k} = \left(\mathcal{B}(\mathrm{e}_n, \mathrm{e}_\ell), \mathrm{e}_k\right), \tag{A 3}$$

with the inner product $(f,g) = \int_{-\pi}^{\pi} f(x)g(x)\,\mathrm{d}x$. In the above equations (A 1) we have assumed the condition $\mathcal{P}_c\mathcal{B}(\mathrm{e}_m,\mathrm{e}_n) = 0$ for the null space, where $n,m = 1,\ldots,N_0$, and we shall also assume the condition $\mathcal{P}_c\mathcal{B}(\mathrm{e}_k,\mathrm{e}_k) = 0$ for the bilinear map, so that we have

$$B_{kkm} = 0, \quad m = 1,\ldots,N_0. \tag{A 4}$$

This assumption, which is satisfied for the Burgers nonlinearity $u\partial_x u$, ensures that the centering condition from homogenisation theory, see Eq. (A 8) below, is satisfied. The system of equations (A 1) for a_m and y_k is of the form of a fast-slow system of stochastic differential equations for which the associated backward-Kolmogorov equation (for $w^\epsilon = \mathbb{E}(f(\boldsymbol{a}(t),\boldsymbol{y}(t)|\boldsymbol{a}(0)=\boldsymbol{a},\boldsymbol{y}(0)=\boldsymbol{y}))$ reads:

$$\partial_t w^\epsilon = (\epsilon^{-2}\mathcal{L}_0 + \epsilon^{-1}\mathcal{L}_1 + \mathcal{L}_2)w^\epsilon, \tag{A 5}$$

where

$$\begin{aligned}
\mathcal{L}_0 &= \sum_{k=N_0+1}^{N}\Big(-\lambda_k y_k\partial_k + \frac{\sigma^2 q_k^2}{2}\partial_k^2\Big),\\
\mathcal{L}_1 &= \sum_{m=1}^{N_0} f_0^m(\boldsymbol{a},\boldsymbol{y})\partial_m + \sum_{k=N_0+1}^{N} g_0^k(\boldsymbol{a},\boldsymbol{y})\partial_k,\\
\mathcal{L}_2 &= \sum_{m=1}^{N_0} f_1^m(\boldsymbol{a})\partial_m + \sum_{k=N_0+1}^{N} g_0^k(\boldsymbol{y})\partial_k,
\end{aligned}$$

and ∂_m and ∂_k represent derivatives respect to a_m and y_k for $m = 1,\ldots,N_0$ and $k = N_0+1,\ldots,N$, respectively. Here, the operator $\mathcal{L}_0$ corresponds to the generator of a finite-dimensional Ornstein-Uhlenbeck (OU) process, so that the invariant measure of the fast process is Gaussian:

$$\rho(d\boldsymbol{y}) = \frac{1}{\mathcal{Z}}\exp\Big(-\sum_{k=N_0+1}^{N}\frac{\lambda_k}{\sigma^2 q_k^2}y_k^2\Big)\mathrm{d}\boldsymbol{y}, \tag{A 7}$$

where $\mathcal{Z}$ is the normalisation constant. From (A 2 *a*) and Assumption (A 4) we deduce

that the vector field $f_0^m(\boldsymbol{a}, \boldsymbol{y})$ is centered with respect to the invariant measure of the fast process,

$$\int_{\mathbb{R}^M} f_0^m(\boldsymbol{a}, \boldsymbol{y})\, \rho(d\boldsymbol{y}) = 0. \tag{A 8}$$

We will now show that the amplitude equation is of the form

$$d\boldsymbol{z} = \bar{\boldsymbol{v}}_M(\boldsymbol{z})\, dt + \bar{\boldsymbol{g}}_M(\boldsymbol{z})\, dW, \tag{A 9}$$

where W denotes a standard N_0-dimensional Wiener process. The subscript M used here is to emphasise the fact that the homogenised coefficients depend on the number of fast processes that we take into account. The calculation of the coefficients $\bar{\boldsymbol{v}}_M(\boldsymbol{z})$ and $\bar{\boldsymbol{g}}_M(\boldsymbol{z})$ which appear in Eq. (A 9) will be obtained by using homogenisation theory.

We solve the backward-Kolmogorov equation (A 5) by looking for a solution in the form of a power series expansion in ϵ:

$$w^\epsilon = w_0 + \epsilon w_1 + \epsilon^2 w_2 + \mathcal{O}(\epsilon^3). \tag{A 10}$$

Substituting this expansion into (A 5) and equating coefficients of powers of ϵ to zero, we find:

$$\mathcal{L}_0 w_0 = 0, \tag{A 11 a}$$

$$\mathcal{L}_0 w_1 + \mathcal{L}_1 w_0 = 0, \tag{A 11 b}$$

$$\mathcal{L}_0 w_2 + \mathcal{L}_1 w_1 + \mathcal{L}_2 w_0 = \partial_t w_0. \tag{A 11 c}$$

Since the null space of the generator of the OU process consists of constant in $\boldsymbol{y}$, from Eq. (A 11 a) we deduce that $w_0 = w_0(\boldsymbol{a}, t)$. The solvability condition for the second

equation reads

$$\int_{\mathbb{R}^M} (\mathcal{L}_1 w_0)\, \rho(d\boldsymbol{y}) = 0. \tag{A 12}$$

This solvability condition is satisfied on account of (A 8), and the fact that the first term in the expansion is independent of $\boldsymbol{y}$. We now solve this equation by using the following ansatz:

$$w_1 = \left(a_m \sum_{\ell=N_0+1}^{N} \chi_{\ell m} y_\ell + \sum_{n,\ell=N_0+1}^{N} \zeta_{n\ell m} y_n y_\ell \right) \partial_m w_0, \tag{A 13}$$

where the constants $\chi_{\ell m}$ and $\zeta_{n\ell m}$ are to be determined from Eq. (A 11 *b*) together with (A 12). In particular, we obtain:

$$\chi_{km} = \frac{2B_{mkm}}{\lambda_k}, \qquad \zeta_{nkm} = \frac{B_{nkm}}{\lambda_n + \lambda_k}, \tag{A 14}$$

for $m = 1, \ldots, N_0$ and $n, k = N_0 + 1, \ldots, N$. Finally, for Eq. (A 11 *c*) we have the solvability condition:

$$\int_{\mathbb{R}^M} \left(\partial_t w_0 - \mathcal{L}_2 w_0 - \mathcal{L}_1 w_1 \right) \rho(d\boldsymbol{y}) = 0, \tag{A 15}$$

which allows us to obtain the homogenised SDE (A 9)[4]. For the components of the drift term we get:

$$v_M^m(\boldsymbol{a}) = \left\langle \left(f_1^m + a_m \sum_{k=N_0+1}^{N} g_0^k \chi_{km} + 2 \sum_{n,k=N_0+1}^{N} g_0^k y_n \zeta_{nkm} + f_0^m \sum_{k=N_0+1}^{N} \chi_{km} y_k \right) \right\rangle, \tag{A 16}$$

for $m = 1, \ldots, N_0$, and where $\langle \ldots \rangle$ denotes average with respect to the invariant measure $\rho(\mathrm{d}\boldsymbol{y})$. Similarly, the components of the quadratic form associated with the diffusion

[4] To be more precise, it allows us to obtain the homogenised backward Kolmogorov equation from which we can read off the limiting SDE.

matrix $\bar{\boldsymbol{g}}_M^2$ are given by:

$$\frac{1}{2}(\bar{g}_M^2)_{ij} = \left\langle f_0^i \left(a_j \sum_{n=N_0+1}^{N} \chi_{nj} y_n + \sum_{n,\ell=N_0+1}^{N} \zeta_{n\ell j} y_n y_\ell \right) \right\rangle, \tag{A 17}$$

where $i, j = 1, \ldots, N_0$. The integrals in (A 16) and (A 17) are Gaussian integrals that can be calculated analytically. In particular, substitution of f_0^i and g_0^i given in Eq. (A 2 *a*) and (A 2 *b*), respectively, into (A 16) and (A 17), and calculation of the resulting Gaussian integrals lead to the amplitude equation (A 9) which can be written as the following system of coupled SL equations:

$$da_m = v_M^m(a_1, \ldots, a_{N_0})dt + \sum_{n=1}^{N_0} (\bar{g}_M)_{mn} dW_n, \tag{A 18}$$

for $m = 1, \ldots, N_0$, and where the different terms are given as:

$$\begin{aligned} v_M^m = & \left(j_m + \sum_{n,k=N_0+1}^{N} \frac{2B_{kmm}B_{nnk}}{\lambda_n \lambda_k} \sigma^2 q_n^2 \right) a_m + \sum_{\ell=1}^{N_0} a_\ell \sum_{n,k=N_0+1}^{N} \frac{2B_{nkm}B_{\ell nk}}{\lambda_n(\lambda_n+\lambda_k)} \sigma^2 q_n^2 \\ & - a_m \sum_{n,\ell=1}^{N_0} a_n a_\ell \sum_{k=N_0+1}^{N} \frac{2B_{kmm}B_{n\ell k}}{\lambda_k}, \end{aligned} \tag{A 19 a}$$

$$\frac{1}{2}(\bar{g}_M^2)_{ij} = a_i a_j \sum_{\ell=1}^{M} \frac{4B_{\ell ii}B_{jnn}}{\lambda_\ell^2} \sigma^2 q_\ell^2 + \sum_{k,n=N_0+1}^{N} \frac{B_{kni}B_{knj}}{\lambda_k(\lambda_n+\lambda_k)^2} \sigma^4 q_n^2 q_k^2. \tag{A 19 b}$$

In the case of a one-dimensional null space ($N_0 = 1$) we define $A = a_1$, and the above expressions have a simpler form. In particular we have:

$$\bar{v}_M(A) = (j_1 + \gamma_1 \sigma^2)A - \gamma_2 A^3, \tag{A 20 a}$$

$$\bar{g}_M(A) = \sigma\sqrt{\gamma_a \sigma^2 + \gamma_m A^2}, \tag{A 20 b}$$

with the different coefficients given as:

$$\gamma_1 = \sum_{n=2}^{N} \frac{2B_{n11}^2}{\lambda_n^2} q_n^2 + \sum_{n,\ell=2}^{N} \frac{2B_{n\ell 1}B_{n1k}}{(\lambda_n+\lambda_\ell)\lambda_n} q_n^2 + \sum_{n,\ell=2}^{N} \frac{B_{n11}B_{nn\ell}}{\lambda_n \lambda_\ell} q_\ell^2, \tag{A 21 a}$$

$$\gamma_2 = \sum_{n=2}^{N} \frac{2B_{n11}B_{11n}}{\lambda_n}, \quad \gamma_a = \sum_{n,\ell=2}^{N} \frac{2B_{n\ell 1}^2}{(\lambda_n+\lambda_\ell)^2 \lambda_\ell} q_n^2 q_\ell^2, \quad \gamma_m = \sum_{n=2}^{N} \frac{4B_{n11}^2}{\lambda_n^2} q_n^2, \tag{A 21 b}$$

where the noise in the resulting amplitude equation is interpreted in the Itô sense. **We note that the form of the amplitude equation (A 20) does not depend on whether the noise is interpreted as Itô or Stratonovich, and the only difference between both interpretations is the first term on the right hand side of the expression for the coefficient γ_1, which exactly corresponds to $\gamma_m/2$, and is a consequence of the multiplicative term of the noise. Let us also remark that the Stratonovich interpretation turns out to be more convenient for the results we present in § 3 for the noisy KS equation, specially for the noise-induced state transitions. Therefore, we will consider the amplitude equation (A 20) with the coefficients given by Eq. (A 21) with $\gamma_1 \to \gamma_1 - \gamma_m/2$.**

It is also interesting to consider the case when the null space is two-dimensional. By assuming the Burgers nonlinearity ($u\partial_x u$), we can explicitly work out the different terms of the amplitude equation (A 18) for the two components $a_1(t)$ and $a_2(t)$, obtaining:

$$v_M^1 = -\frac{1}{4\lambda_2}a_1^3 - \frac{1}{4\lambda_2}a_1a_2^2 + \big(j_1 + V_M\big)a_1, \tag{A 22 a}$$

$$v_M^2 = -\frac{1}{4\lambda_2}a_2^3 - \frac{1}{4\lambda_2}a_1^2a_2 + \big(j_2 + V_M\big)a_2, \tag{A 22 b}$$

$$\frac{1}{2}(\bar{g}_M^2) = \begin{pmatrix} \frac{\sigma^2}{8}\frac{r_2^2a_2^2}{\lambda_2^2} + \frac{\sigma^2}{8}\frac{q_2^2a_1^2}{\lambda_2^2} + G_M & \frac{\sigma^2}{8}\frac{(r_2^2-q_2^2)}{\lambda_2^2}a_1a_2 \\ \frac{\sigma^2}{8}\frac{(r_2^2-q_2^2)}{\lambda_2^2}a_1a_2 & \frac{\sigma^2}{8}\frac{r_2^2a_1^2}{\lambda_2^2} + \frac{\sigma^2}{8}\frac{q_2^2a_2^2}{\lambda_2^2} + G_M \end{pmatrix}, \tag{A 22 c}$$

with the coefficients:

$$V_M = \frac{\sigma^2}{8}\sum_{k=2}^{M}\frac{k\lambda_k(q_{k+1}^2 + r_{k+1}^2) - \lambda_{k+1}(q_k^2 + r_k^2)(k+1)}{(\lambda_{k+1}+\lambda_k)\lambda_k\lambda_{k+1}},$$

$$G_M = \frac{\sigma^4}{16}\sum_{k=2}^{M}\frac{q_k^2q_{k+1}^2 + r_k^2r_{k+1}^2}{\lambda_k(\lambda_{k+1}+\lambda_k)\lambda_{k+1}},$$

where we have assumed a general case where the two components of the noise for each fast

mode (which arise as a consequence of the fact that the null space is multidimensional) have different wave number dependence, namely q_k and r_k. We therefore see that in general, the diffusion matrix is non diagonal and the resulting amplitude equations are coupled not only through the drift term but also through the noise term.

Appendix B Derivation of the noisy Kuramoto–Sivashinsky equation for a hydrodynamic system

We provide a physical example where the noisy KS equation can be derived from a general formulation in the framework of thin-film hydrodynamics.

Consider gravity-driven thin film flow down an uneven wall that is inclined at an angle θ to the horizontal, as shown in Fig. B 1. Let x and z be the stream- and the cross-stream coordinates, respectively, and the wall be described by $z = s(x,t)$ relative to a datum plane and where the time-dependence is such that each point of the wall fluctuates only in the z-direction, i.e., at a given time t the velocity of the wall point $(x, s(x,t))$ is the vector $(0, s_t(x,t))$. Let also the free surface be located at $z = f(x,t)$. We introduce dimensionless variables by utilising the Nusselt film thickness h_0 (corresponding to undisturbed flow down an inclined plane) as a lengthscale, the Nusselt surface velocity $U_0 = \rho g h_0^2 \sin\theta/2\mu$, where ρ and μ are the density and the dynamic viscosity of the liquid, respectively, and g is gravity, as a velocity scale and U_0/h_0 as a time scale. The pressure scale is chosen as $\mu U_0/h_0$. We additionally introduce the Reynolds number $Re = \rho U_0 h_0/\mu$ and the capillary number $Ca = \mu U_0/\gamma$ where γ denotes the surface tension.

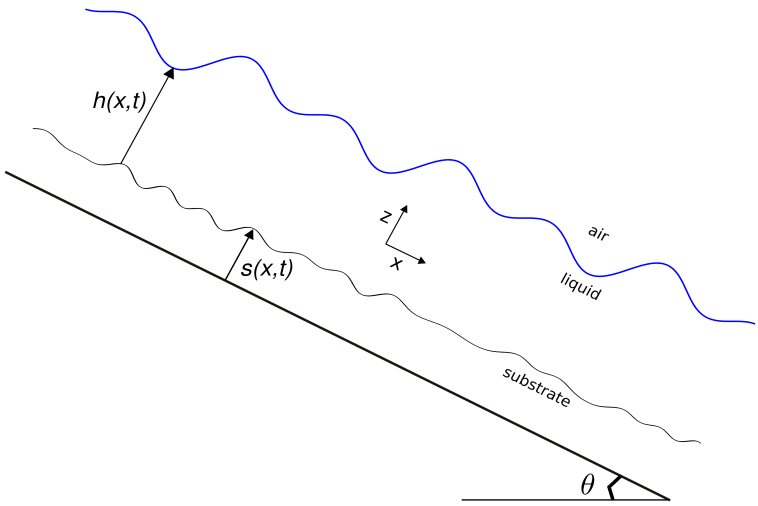

FIGURE B 1. Sketch of a liquid film falling down over an inclined plane with a vibrating disordered wall. The thickness of the film and the disordered wall position are denoted as $h(x,t)$ and $s(x.t)$, respectively.

The governing equations are given by the incompressible Navier–Stokes equations:

$$Re(u_t + uu_x + vu_z) = -p_x + u_{xx} + u_{zz} + 2, \tag{B 1}$$

$$Re(v_t + uv_x + vv_z) = -p_z + v_{xx} + v_{zz} - 2\cot\theta, \tag{B 2}$$

$$u_x + v_z = 0, \tag{B 3}$$

where subindices represent partial derivatives, u and v denote the x- and the z-component of the velocity in the liquid, respectively, and p denotes the deviation of the pressure from the atmospheric level. The boundary conditions at the wall, $z = s(x,t)$, are given by:

$$u = 0, \qquad v = s_t(x,t), \tag{B 4}$$

and at the free surface, $z = f(x,t)$, the kinematic compatibility and the tangential and

normal stress balance conditions are satisfied:

$$f_t + uf_x - v = 0, \tag{B 5}$$

$$(1 - f_x^2)(u_z + v_x) + 2f_x(v_z - u_x) = 0, \tag{B 6}$$

$$p = \frac{2}{1 + f_x^2}(-f_x(u_z + v_x) + u_x f_x^2 + v_z) - \frac{f_{xx}}{Ca(1 + f_x^2)^{3/2}}. \tag{B 7}$$

We consider here the long-wave approximation so that we introduce the so-called thin-film or long-wave parameter ε, defined as the ratio of the typical film thickness to the length scale over which streamwise variations occur. We then introduce new variables: $\xi = \varepsilon x$, $\tau = \varepsilon t$, and $w = v/\varepsilon$. We also assume that $Ca = O(\varepsilon^2)$ and define $\widetilde{C}a = Ca/\varepsilon^2$. We expand the different variables as, $u = u_0 + \varepsilon u_1 + \cdots$, $w = w_0 + \varepsilon w_1 + \cdots$, and $p = p_0 + \varepsilon p_1 + \cdots$, which lead to a series of solvable perturbation problems. The leading-order problem is:

$$u_{0zz} = 0, \qquad p_{0z} = -2\cot\theta, \qquad u_{0\xi} + w_{0z} = 0. \tag{B 8}$$

At $z = s(\xi, \tau)$, $u_0 = 0$, $w_0 = s_\tau(\xi, \tau)$. At the free surface, $z = f(\xi, \tau)$, the tangential and normal stress balance conditions imply $u_{0z} = 0$, $p_0 = -f_{\xi\xi}/\widetilde{C}a$. The solution of the problem at leading order is:

$$u_0 = -(z - h - s)^2 + h^2, \tag{B 9}$$

$$w_0 = u_0(h + s)_\xi - [h^2]_\xi(z - s) + s_\tau(\xi, \tau), \tag{B 10}$$

$$p_0 = -2(\cot\theta)(z - h - s) - (h + s)_{\xi\xi}/\widetilde{C}a, \tag{B 11}$$

where we introduced for convenience the film thickness $h = f - s$. Note that the kinematic compatibility condition can be written as

$$h_\tau + q_\xi = 0, \tag{B 12}$$

where $q = \int_s^f u \, \mathrm{d}z$. Using (B 9), we find $q = \frac{2}{3}h^3 + O(\varepsilon)$, which implies

$$h_\tau + \left[\tfrac{2}{3}h^3\right]_\xi + O(\varepsilon) = 0. \tag{B 13}$$

At next order, we obtain the following system of equations:

$$u_{1zz} = Re(u_{0\tau} + u_0 u_{0\xi} + w_0 u_{0z}) + p_{0\xi}, \tag{B 14}$$

$$p_{1z} = w_{0z}, \tag{B 15}$$

$$u_{1\xi} + w_{1z} = 0, \tag{B 16}$$

subject to $u_1 = w_1 = 0$ at $z = s$ and $u_{1z} = 0$, $p_1 = 2w_{0z} - 2f_\xi u_{0z}$ at $z = f$, where u_0, w_0, and p_0 are given by (B 9)–(B 11). The time derivative $u_{0\tau}$ involves the time derivative h_τ, as is evident from (B 9). The latter is eliminated by using (B 13). For brevity we do not show the solution of the problem at first order (which can be easily found with a symbolic manipulation software) as it turns out to be rather lengthy. Substituting $u = u_0 + \varepsilon u_1 + O(\varepsilon^2)$ into $q = \int_s^f u \, \mathrm{d}z$, we find

$$q = \frac{2}{3}h^3 + \varepsilon h^3 \left[\frac{8Re}{15}h^3 h_\xi - \frac{2\cot\theta}{3}(h+s)_\xi + \frac{1}{3\widetilde{Ca}}(h+s)_{\xi\xi\xi}\right] + O(\varepsilon^2).$$

Thus, we obtain the following evolution equation for the film thickness, h:

$$h_\tau + \left(\frac{2}{3}h^3 + \varepsilon h^3 \left[\frac{8Re}{15}h^3 h_\xi - \frac{2\cot\theta}{3}(h+s)_\xi + \frac{1}{3\widetilde{Ca}}(h+s)_{\xi\xi\xi}\right]\right)_\xi = 0. \tag{B 17}$$

We proceed next with a weakly nonlinear analysis. We assume that both the amplitude of the free surface and the bottom wall are small, of $O(\varepsilon)$, and we write $h = 1 + \varepsilon\eta$ and $s = \varepsilon\sigma$. Substituting these expressions into the evolution equation above re-written in the moving frame, $\chi = \xi - 2\tau$, we obtain the following evolution equation:

$$\bar{\eta}_{\bar{\tau}} + 4\bar{\eta}\bar{\eta}_\chi + D\bar{\eta}_{\chi\chi} + \frac{1}{3\widetilde{Ca}}\bar{\eta}_{\chi\chi\chi\chi} = \Sigma, \tag{B 18}$$

where $O(\varepsilon^2)$ terms have been neglected, $\tilde{\tau} = \varepsilon\tau$, $\bar{\eta}(\chi, \tilde{\tau}) = \eta(\chi + 2\tilde{\tau}/\varepsilon, \tilde{\tau}/\varepsilon)$, $\bar{\sigma}(\chi, \tilde{\tau}) = \sigma(\chi + 2\tilde{\tau}/\varepsilon, \tilde{\tau}/\varepsilon)$, $D = 8Re/15 - 2\cot\theta/3$ and $\Sigma = (2\cot\theta/3)\bar{\sigma}_{\chi\chi} - (1/3\widetilde{C}a)\bar{\sigma}_{\chi\chi\chi\chi}$. We find that $s(\xi, \tau) = \epsilon\bar{\sigma}(\xi - 2\tau, \epsilon\tau)$, which physically means that the typical deformation of the topography shape is of small amplitude and large wavelength (of the same order as the wavelength of the typical free-surface wave), it propagates downstream with constant velocity, and is slowly changing in the frame moving with this velocity.

To simplify the latter evolution equation, we introduce the transformation, $\bar{\eta} = U/A$, $\chi = X/B$, and $\tilde{\tau} = T/C$, where $A = 4/(3\widetilde{C}a|D|^3)^{1/2}$, $B = (3\widetilde{C}a|D|)^{1/2}$, and $C = 3\widetilde{C}aD^2$, which leads to the following canonical form:

$$U_T + UU_X \pm U_{XX} + U_{XXXX} = S(X, T), \tag{B 19}$$

where $S = (A/C)\Sigma$, and the sign $+/-$ corresponds to the positive/negative value of D. We therefore obtain the noisy KS equation (3.1).

Acknowledgements. We acknowledge financial support from EU-FP7 ITN Grant No. 214919 (Multiflow), ERC Advanced Grant No. 247031 and the EPSRC Grant No. EP/H034587/1. The work of DTP was also supported in part by the National Science Foundation grant DMS-0707339.

References

[1] Barabási, A.-L. & Stanley, H. E. (1995) *Fractal Concepts in Surface Growth*. Cambridge University Press, Cambridge, England.

[2] Bezrukov, S. M. & Vodyanoy, I. (1995) Noise-induced enhancement of signal transduction across voltage-dependent ion channels. *Nature (London)* **378**, 362–364.

[3] Blömker, D. (2007) *Amplitude equations for stochastic partial differential equations*, *Interdisciplinary Mathematical Sciences*, vol. 3. World Scientific Publishing Co. Pte. Ltd., Hackensack, NJ.

[4] Blömker, D., Hairer, M. & Pavliotis, G.A. (2009) Some remarks on stabilization by additive noise. *Preprint* .

[5] Blömker, D., Hairer, M. & Pavliotis, G. A. (2007) Multiscale analysis for stochastic partial differential equations with quadratic nonlinearities. *Nonlinearity* **20**, 1721–1744.

[6] Blömker, D. & Mohammed, W. W. (2009) Amplitude equation for SPDEs with quadratic nonlinearities. *Electron. J. Probab.* **14**, no. 88, 2527–2550.

[7] Cross, M. C. & Hohenberg, P. C. (1993) Pattern formation outside of equilibrium. *Rev. Mod. Phys.* **65**, 851–1112.

[8] Cuerno, A., Makse, H. A., Tomassone, S., Harrington, S. T. & Stanley, H. E. (1995) Stochastic erosion for surface erosion via ion sputtering: Dynamical evolution from ripple morphology to rough morphology. *Phys. Rev. Lett.* **75**, 4464–4467.

[9] Cuerno, R. & Barabási, A.-L. (1995) Dynamic scaling of ion-sputtered surfaces. *Phys. Rev. Lett.* **74**, 4746.

[10] Duan, J. & Ervin, V. J. (2001) On the stochastic Kuramoto-Sivashinsky equation. *Nonlinear Analysis* **44**, 205–216.

[11] Duprat, C., Giorgiutti-Dauphiné, F., Tseluiko, D., Saprykin, S. & Kalliadasis, S. (2009) Liquid film coating a fiber as a model system for the formation of bound states in active dispersive-dissipative nonlinear media. *Phys. Rev. Lett.* **103**, 234501.

[12] Frost, F. & Rauschenbach, B. (2003) Nanostructuring of solid surfaces by ion beam erosion. *Appl. Phys. A* **77**, 1–9.

[13] García-Ojalvo, J., Hernández-Machado, A. & Sancho, J. M. (1993) Effects of external noise on the Swift-Hohenberg equation. *Phys. Rev. Lett.* **71**, 1542–1545.

[14] García-Ojalvo, J. & Sancho, J. M. (1999) *Noise in Spatially Extended Systems*. Springer-Verlag, New York.

[15] Heagy, J. F., Platt, N. & Hammel, S. M. (1994) Characterization of on-off intermittency. *Phys. Rev. E* **49**, 1140–1150.

[16] Horsthemke, W. & Lefever, R. (1984) *Noise-Induced Transitions*. Springer, Berlin.

[17] Hutt, A. (2008) Additive noise may change the stability of nonlinear systems. *Europhysics Lett.* **84**, 34003.

[18] Hutt, A., Longtin, A. & Schimansky-Geier, L. (2007) Additive global noise delays turing bifurcations. *Phys. Rev. Lett.* **98**, 230601.

[19] Hyman, J. M. & Nicolaenko, B. (1986) The Kuramoto–Sivashinsky equation: a bridge between PDEs and dynamical systems. *Phys. D* **18**, 113–126.

[20] Hyman, J. M., Nicolaenko, B. & Zaleski, S. (1986) Order and complexity in the Kuramoto–Sivashinsky model of weakly turbulent interfaces. *Phys. D* **23**, 265–292.

[21] John, T., Stannarius, R. & Behn, U. (1999) On-off intermittency in stochastically driven electrohydrodynamic convection in nematics. *Phys. Rev. Lett.* **83**, 749–752.

[22] Jolly, M. S., Kevrekidis, I. G. & Titi, E. S. (1990) Approximate inertial manifolds for the Kuramoto–Sivashinsky equation: analysis and computations. *Phys. D* **44**, 38–60.

[23] Kalliadasis, S. & Thiele, U. (Eds.) (2007) *Thin Films of Soft Matter*. Springer-Wien, CISM.

[24] Karma, A. & Misbah, C. (1993) Competition between noise and determinism in step flow growth. *Phys. Rev. Lett.* **71**, 3810.

[25] Kuramoto, Y. & Tsuzuki, T. (1976) Persistent propagation of concentration waves in dissipative media far from thermal equilibrium. *Prog. Theor. Phys.* **55**, 356–369.

[26] Landa, P. S., Zaikin, A. A. & Schimansky-Geier, L. (1998) Influence of additive noise on noise-induced phase transitions in nonlinear chains. *Chaos, Solitons & Fractals* **9**, 1367–1372.

[27] Lauritsen, K. B., Cuerno, A. & Makse, H. A. (1996) Noisy Kuramoto–Sivashinsky equation for an erosion model. *Phys. Rev. E* **54**, 3577–3580.

[28] López, J. M., Pradas, M. & Hernández-Machado, A. (2010) Activity statistics, avalanche kinetics, and velocity correlations in surface growth. *Phys. Rev. E* **82**, 031127.

[29] Lou, Y. & Christofides, P. D. (2005) Feedback control of surface roughness in sputtering processes using the stochastic Kuramoto–Sivashinsky equation. *Computers & Chemical Engineering* **29**, 741–759.

[30] Lou, Y., Hu, G. & Christofides, P. D. (2008) Model predictive control of nonlinear stochastic partial differential equations with application to a sputtering process. *AIChE Journal* **54**, 2065–2081.

[31] Mackey, M. C., Longtin, A. & Lasota, A. (1990) Noise-induced global asymptotic stability. *J. Stat. Phys.* **60**, 735–751.

[32] Majda, A. J., Timofeyev, I. & Eijnden, E. Vanden (2001) A mathematical framework for stochastic climate models. *Comm. Pure Appl. Math.* **54** (8), 891–974.

[33] Mecke, K. & Rauscher, M. (2005) On thermal fluctuations in thin film flow. *J. Phys.: Condens. Matter* **17**, S3515–S3522.

[34] Obeid, D., Kosterlitz, J. M. & Sandstede, B. (2010) State selection in the noisy stabilized Kuramoto-Sivashinsky equation. *Phys. Rev. E* **81**, 066205.

[35] Papageorgiou, D. T., Maldarelli, C. & Rumschitzki, D. S. (1990) Nonlinear interfacial stability of core-annular film flows. *Phys. Fluids A* **2**, 340–352.

[36] Papageorgiou, D. T. & Smyrlis, Y.-S. (1991) The route to chaos for the Kuramoto–Sivashinsky equation. *Theoret. Comput. Fluid Dynamics* **3**, 15–42.

[37] Papanicolaou, G. C. (1976) Some probabilistic problems and methods in singular perturbations. *Rocky Mountain J. Math.* **6** (4), 653–674.

[38] Pavliotis, G. A. & Stuart, A. M. (2008) *Multiscale Methods: Averaging and Homogenization*. Springer, New York.

[39] Platt, N., Spiegel, E. A. & Tresser, C. (1993) On-off intermittency: a mechanism for bursting. *Phys. Rev. Lett.* **70**, 279–282.

[40] Pradas, M., López, J. M. & Hernández-Machado, A. (2009) Avalanche dynamics in fluid imbibition near the depinning transition. *Phys. Rev. E* **80**, 050101(R).

[41] Pradas, M., Tseluiko, D., Kalliadasis, S., Papageorgiou, D. T. & Pavliotis, G. A. (2011) Noise induced state transitions, intermittency, and universality in the noisy Kuramoto-Sivashinsky equation. *Phys. Rev. Lett.* **106** (6), 060602.

[42] Pradas, M., Tseluiko, D. & Kalliadasis (2011) Rigorous coherent-structure theory for falling liquid films: Viscous dispersion effects on bound-state formation and self-organization. *Phys. Fluids* **23**, 044104.

[43] Redner, S. (2001) *A Guide to First-Passage Processes*. Cambridge University Press, Cambridge, England.

[44] Roberts, A. J. (2003) A step towards holistic discretisation of stochastic partial differential equations. *ANZIAM J.* **45** ((C)), C1–C15.

[45] Sagués, F., Sancho, J. M. & García-Ojalvo, J. (2007) Spatiotemporal order out of noise. *Rev. Mod. Phys.* **79**, 829–882.

[46] Saprykin, S., Demekhin, E. A. & Kalliadasis, S. (2005) Two-dimensional wave dynamics in thin films. i. stationary solitary pulses. *Phys. Fluids* **17**, 117105.

[47] Shew, W. L., Yang,H., Petermann, T., Roy, R. & Plenz, D. (2009) Neuronal avalanches imply maximum dynamic range in cortical networks at criticality. *J. Neurosci.* **29**, 15595.

[48] Sivashinsky, G. I. (1977) Nonlinear analysis of hydrodynamic instability in laminar flames: I.derivation of basic equations. *Acta Astraunaut.* **4**, 1176–1206.

[49] Smyrlis, Y.-S. & Papageorgiou, D. T. (1991) Predicting chaos for infinite–dimensional dynamical systems: the Kuramoto–Sivashinsky equation, a case study. *Proc. Nat. Acad. Sci. U.S.A.* **88**, 11129–11132.

[50] Tseluiko, D., Saprykin, S., Duprat, C., Giorgiutti-Dauphiné, F. & Kalliadasis, S. (2010) Pulse dynamics in low-Reynolds number interfacial hydrodynamics: Experiments and theory. *Physica D* **239**, 2000–2010.

[51] Wan, X., Zhou, X. & E, W. (2010) Study of the noise-induced transition and the exploration of the phase space for the Kuramoto-Sivashinsky equation using the minimum action method. *Nonlinearity* **23**, 475–493.

[52] Wiesenfeld, K. & Moss, F. (1995) Stochastic resonance and the benefits of noise: from ice ages to crayfish and SQUIDs. *Nature (London)* **373**, 33–36.

[53] Wittenberg, R. W. (2002) Dissipativity, analyticity and viscous shocks in the (de)stabilized Kuramoto–Sivashinsky equation. *Phys. Lett. A* **300**, 407–416.

[54] Wittenberg, R. W. & Holmes, P. (1999) Scale and space localization in the Kuramoto–Sivashinsky equation. *Chaos* **9**, 452–464.

[55] Wylock, C., Pradas, M., Haut, B., Colinet, P. & Kalliadasis, S. (2012) Disorder-induced hysteresis and nonlocality of contact line motion in chemically heterogeneous microchannels. *Phys. Fluids* **24**, 032108.

[56] Zaikin, A. A., García-Ojalvo, J. & Schimansky-Geier, L. (1999) Nonequilibrium first-order phase transition induced by additive noise. *Phys. Rev. E* **9**, R6275–R6278.